

Adversarial Neon Beam: A Light-based Physical Attack to DNNs

Chengyin Hu

University of Electronic Science and
Technology of China
Chengdu, China
cyhuuesct@gmail.com

Weiwen Shi

University of Electronic Science and
Technology of China
Chengdu, China
weiwen_shi@foxmail.com

Wen Li*

University of Electronic Science and
Technology of China
Chengdu, China
liwen@uestc.edu.cn

ABSTRACT

In the physical world, deep neural networks (DNNs) are impacted by light and shadow, which can have a significant effect on their performance. While stickers have traditionally been used as perturbations in most physical attacks, their perturbations can often be easily detected. To address this, some studies have explored the use of light-based perturbations, such as lasers or projectors, to generate more subtle perturbations, which are artificial rather than natural. In this study, we introduce a novel light-based attack called the adversarial neon beam (**AdvNB**), which utilizes common neon beams to create a natural black-box physical attack. Our approach is evaluated on three key criteria: effectiveness, stealthiness, and robustness. Quantitative results obtained in simulated environments demonstrate the effectiveness of the proposed method, and in physical scenarios, we achieve an attack success rate of 81.82%, surpassing the baseline. By using common neon beams as perturbations, we enhance the stealthiness of the proposed attack, enabling physical samples to appear more natural. Moreover, we validate the robustness of our approach by successfully attacking advanced DNNs with a success rate of over 75% in all cases. We also discuss defense strategies against the AdvNB attack and put forward other light-based physical attacks.

KEYWORDS

DNNs; light-based attack; AdvNB; Effectiveness; Stealthiness; Robustness.

1 INTRODUCTION

Deep learning has demonstrated remarkable achievements in various fields, even surpassing human-level performance [1–3]. As a result, it has been extensively employed in applications such as autonomous vehicles [4, 5], robotics [6], and UAVs [7, 8]. However, deep neural networks (DNNs) are vulnerable to well-crafted adversarial perturbations [9–11], leading to unpredictable aberrant behavior in vision-based systems. For instance, in autonomous driving, an attack on DNNs could result in car crashes. Adversarial attacks have mainly been investigated in the digital domain [12–15], where subtle perturbations are intentionally added to input images, making them difficult for human observers to detect. Recently, some researchers have focused on physical adversarial attacks [16–19], which involve capturing images by a camera and then feeding them to the target model. Physical perturbations are typically designed to be visible so that they can be captured by the camera, yet at the same time, they need to be inconspicuous enough to avoid detection

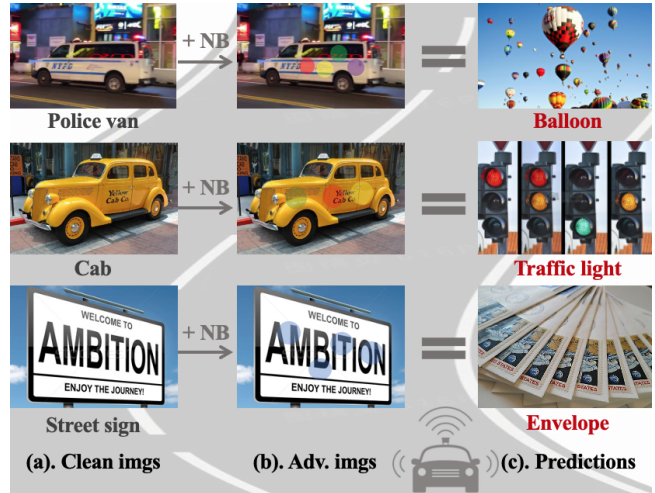


Figure 1: An example. When the camera of a self-driving system captures objects illuminated by neon beams, it may fail to recognize them accurately.

by human observers. Therefore, physical attacks typically involve a trade-off between stealthiness and robustness.

Numerous natural phenomena can serve as physical perturbations. In urban areas, in particular, neon beams are ubiquitous and often scatter onto traffic signs, leading humans to unconsciously disregard them. However, if an attacker intentionally generates adversarial neon beams to fool self-driving car systems while lowering human vigilance, it could severely disrupt traffic flow. As illustrated in Figure 1, an adversary can project ingeniously crafted adversarial neon beams onto a road sign, leading advanced DNNs to misclassify it.

The investigation of the adversarial impact of light-based physical attacks on advanced DNNs is of great significance. Currently, most physical attacks employ stickers as perturbations [20, 21], which successfully deceive advanced DNNs without altering the semantic information of the target objects. However, sticker-based attacks entail affixing stickers or posters onto the surface of the target object, which lacks flexibility and makes it difficult to achieve stealthiness. Additionally, some researchers have examined camera-based adversarial attacks [22], in which some tiny translucent patches are placed on the camera of a mobile phone to perform physical attacks. However, adding too many patches can result in experimental errors. Recently, some scholars have used light beams as physical perturbations [23, 24] to conduct instantaneous attacks, which effectively

*Corresponding authors



Figure 2: Visual comparison.

deceive advanced DNNs and offer better stealthiness. However, this method is prone to failure during daylight hours.

In this work, we present a light-based physical attack called Adversarial Neon Beam (AdvNB). Unlike existing sticker-based attacks, our method employs the instantaneous attack nature of neon beams to execute physical attacks, rendering it more flexible and stealthy. Compared to other light-based methods, our approach is more natural and offers enhanced stealthiness. A visual comparison of our method with other works is depicted in Figure 2. The adversarial samples generated by AdvNB are significantly stealthier than those generated by other methods such as RP2 [20], AdvLB [23], and shadow attack [25].

Our proposed method offers a straightforward implementation for physical attacks. We formalize the physical parameters of the neon beam, including the radius, intensity, color, and center position. Then, we design an optimization method to search for the most adversarial physical parameters. To achieve the transition from the digital domain to the physical domain, we employ EOT [26]. Finally, based on these physical parameters, we project physical neon beams onto the target objects to generate physical samples. Notably, our approach enables low-cost attacks, requiring a budget of less than 50 USD, which significantly facilitates deployment. Our main contributions can be summarized as follows:

- We introduce a novel light-based physical attack method, AdvNB, that exploits the instantaneous nature of neon beams to manipulate their physical parameters and generate black-box physical attacks (see section 1). Our approach is effective and low-cost, making it significantly easier to deploy.
- We introduce and analyze the existing methods (See section 2), analyze the advantages of our approach over traditional road sign attacks and the existing light-based attacks. Then, we design strict experimental method and conduct comprehensive experiments to verify the effectiveness, stealthiness and robustness of AdvNB (See section 3, 4). Our results indicate that AdvNB is capable of achieving high success rates while remaining inconspicuous to the naked eye, even in challenging real-world scenarios. Given these findings, we believe

that AdvNB represents a valuable tool for further studying the threat posed by light-based attacks in realistic settings.

- We perform a comprehensive analysis of AdvNB, which includes studying the impact of AdvNB on DNNs’ prediction errors, and investigating the defense strategies against AdvNB (as detailed in section 5). These investigations serve to facilitate scholars in exploring and defending against light-based physical attacks. Moreover, we also examine some potential avenues for future research on light-based physical attacks (as discussed in section 6).

2 RELATED WORK

2.1 Digital attacks

The concept of adversarial attacks was initially introduced by Szegedy et al. [9], and subsequently, many digital attacks have been proposed [27–30].

Currently, many digital attacks aim to ensure that perturbations are imperceptible to human observers by confining them to a norm-ball, with L_2 and L_∞ being the most frequently employed norms [31, 32]. These methods have proven to be effective in attacking advanced deep neural networks while maintaining the perturbations’ imperceptibility to humans. Other works have focused on modifying other characteristics of clean samples for adversarial attacks, such as color [33–35], texture, and camouflage [36–39], which are often noticeable to the naked eye. Additionally, some research has generated adversarial samples by manipulating the physical parameters of clean images, while retaining the critical components of the images, thus facilitating digital attacks [40, 41]. Several works [42, 43] have proposed the raindrop attack, which employs simulated raindrops as perturbations, to test its attack effectiveness and subsequently develop defense mechanisms for obtaining robust deep neural networks. In contrast to digital attacks, physical attacks cannot directly manipulate input images.

2.2 Physical attacks

Physical attack was first proposed by Alexey Kurakin et al. [44]. After this work, many physical attacks were proposed successively [26, 45–47].

Traditional street sign attacks. Ivan Evtimov et al. [20] proposed RP2, which demonstrated a robust adversarial effect against advanced deep neural networks. However, RP2 is vulnerable to environmental interference at large distances and angles. Eykholt et al. [21] improved RP2 and employed the attack on a target detector, resulting in the detector disregarding the target object. However, the perturbations cover an extensive area, they are too conspicuous. Chen et al. [48] proposed ShapeShifter, which overcame the non-differentiability of the Faster R-CNN model, and successfully executed optimization-based attacks using gradient descent and back propagation. Huang et al. [49] further enhanced ShapeShifter by adding Gaussian white noise to its optimization function, addressing ShapeShifter’s high requirements for photographic equipment. However, both ShapeShifter and its improved version have a limitation: the perturbations cover almost the entire road sign, making them non-stealthy. Duan et al. [50] proposed AdvCam, which leverages style transfer techniques to generate adversarial samples and disguise perturbations as a style that humans would consider reasonable.

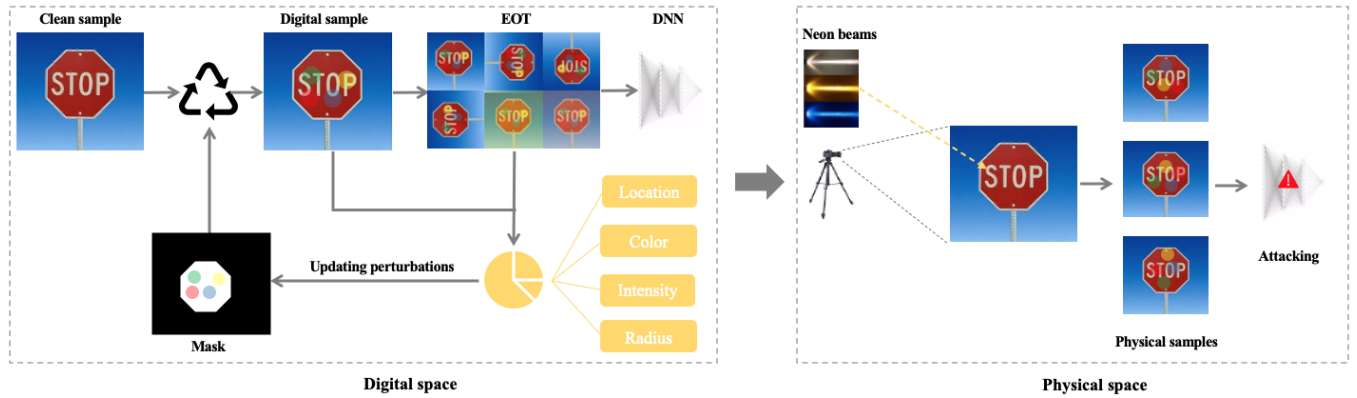


Figure 3: Generating adversarial samples.

However, AdvCam requires manual selection of the attack area and target and suffers from printing losses. In general, traditional road sign attacks have significant drawbacks: adding physical perturbations is a manual and time-consuming process, while also susceptible to printing errors.

Light-based attacks. Light-based attacks have shown some advantages over traditional street sign attacks. For instance, Duan et al. [23] proposed AdvLB, which allows for manipulations of the physical parameters of laser beams to perform physical attacks. However, AdvLB is prone to spatial errors. To address this limitation, Gnanasambandam et al. [51] proposed OPAD, which projects digital perturbations onto the target objects to perform physical attacks on advanced DNNs. However, OPAD is prone to paralyzation during daytime conditions. Another physical attack approach is shadow-based physical attack, as studied by Zhong et al. [25], who use carefully crafted shadows as physical perturbations to generate physical samples and conduct effective attacks on advanced DNNs. However, the cardboard used in this approach is placed too close to the target objects, which may raise suspicions among human observers.

Raindrop-based attacks. Additionally, Guesmi et al. [52] proposed Advrain, which performs physical attacks by simulating real raindrops. They achieved an average model accuracy reduction of 45% for VGG19 and 40% for ResNet34 using 20 raindrops. AdvRain implements stealthy physical attacks, but its robustness still needs to be explored.

3 APPROACH

Given an input image X , a ground truth label Y , and a DNN classifier f , $f(X)$ represents the classifier’s prediction label, the classifier f associates with a confidence score $f_Y(X)$ to class Y . Generating adversarial sample X_{adv} satisfies two properties : (1) $f(X_{adv}) \neq f(X) = Y$; (2) $\|X_{adv} - X\| < \epsilon$. The first one requires that X_{adv} successfully fool DNN classifier f , and the second one ensures the adversarial perturbations to be imperceptible to human observers.

Figure 3 illustrates our proposed method, AdvNB. Firstly, we simulate neon beams and synthesize them with clean images to generate digital samples. Then, we use EOT [26] to transition from the digital domain to the physical domain, followed by projecting

the physical neon beams onto the target object to generate physical samples.

3.1 Generating adversarial sample

In our study, we define a neon beam by considering four key parameters: center position denoted by $L(m, n)$, radius represented by R , intensity denoted by I , and color represented by $C(r, g, b)$. Each parameter is defined as follows:

Position $L(m, n)$: We define the center position of the neon beam as $L(m, n)$. The neon beam is assumed to be circular and represented by a double tuple (m, n) to indicate its center position.

Radius R : R represents the radius of neon beam.

Beam intensity I : The parameter I determines the strength of the neon beam projected onto the target object, with larger values indicating greater intensity and brighter illumination.

Colors $C(r, g, b)$: The parameter $C(r, g, b)$ determines the color of the neon beam. Here, r , g , and b represent the intensity of the red, green, and blue channels of a digital image, respectively. In the physical environment, due to equipment limitations, we have chosen to use five common colors: Red $C(225, 0, 0)$, Green $C(0, 255, 0)$, Blue $C(0, 0, 255)$, Yellow $C(255, 255, 0)$, and Purple $C(255, 0, 255)$.

The aforementioned parameters collectively define a neon beam $\theta(L, R, I, C)$, and the neon beams are grouped as \mathcal{G}_θ , with each parameter having an adjustable range. \mathcal{M} is defined as the mask to locate the target objects, and the neon beams present in the target objects are given by $\mathcal{M} \cap \mathcal{G}_\theta$. The proposed AdvNB aims to identify the neon beam group \mathcal{G}_θ that causes the simulated adversarial sample X_{adv} to be misclassified by the target model f . To constrain the physical parameters L , R , I , and C within appropriate ranges, we define the restriction vectors ϑ_{min} and ϑ_{max} , which are adjustable. The adversarial example generation process can be denoted as:

$$X_{adv} = S(X, \mathcal{G}_\theta, \mathcal{M}) \quad \theta \in (\vartheta_{min}, \vartheta_{max}) \quad (1)$$

where X_{adv} denotes adversarial samples and S denotes simple linear fusion method to fuse clean sample X and \mathcal{G}_θ .

Expectation Over Transformation. In order to launch a successful physical-world attack, it is necessary to transform the digital samples into physical samples. Expectation Over Transformation

(EOT) [26] is a widely used method for this purpose, which ensures the generation of robust physical samples that can withstand various transformations, such as different distances and angles. We define a transformation function \mathcal{T} to represent the domain transition, which is a random combination of digital image processing techniques, such as brightness adaptation, position offset, and color variation. By applying EOT, the physical sample can be expressed as:

$$X_{phy} = \mathcal{T}(X_{adv}, \mathcal{G}_\theta) \quad \theta \in (\vartheta_{min}, \vartheta_{max}) \quad (2)$$

Algorithm 1 Pseudocode of AdvNB

Input: Input X , Ground truth label Y , Max step t_{max} , The number of neon beams N , Classifier f ;
Output: A vector of parameters \mathcal{G}_θ ;

- 1: **Initialization** $\mathcal{G}_\theta = \emptyset, \theta = \emptyset, \theta_{opt} = \emptyset$;
- 2: $Score^* \leftarrow f_Y(X)$;
- 3: **for** $i \leftarrow 0$ to N **do**
- 4: **for** step $\leftarrow 0$ to t_{max} **do**
- 5: Randomly pick L, R, I, C ;
- 6: $\theta = \theta(L, R, I, C)$;
- 7: $X_{adv} = S(X_{adv}, \theta, \mathcal{M})$;
- 8: $f_Y(X_{adv}) \leftarrow f(X_{adv})$;
- 9: **if** $Score^* > f_Y(X_{adv})$ **then**
- 10: $Score^* \leftarrow f_Y(X_{adv})$;
- 11: $\theta_{opt} = \theta$;
- 12: **end if**
- 13: **end for**
- 14: $\mathcal{G}_\theta \leftarrow \mathcal{G}_\theta + \theta_{opt}$;
- 15: $X_{adv} = S(X, \mathcal{G}_\theta, \mathcal{M})$;
- 16: **end for**
- 17: **if** $argmax f(X_{adv}) \neq argmax f(X)$ **then**
- 18: **Return** \mathcal{G}_θ ;
- 19: **end if**

3.2 Neon beam adversarial attack

AdvNB focuses on searching \mathcal{G}_θ , the physical parameters of adversarial neon beams, which generates an adversarial sample X_{adv} that fools the target model f . In our test, we consider an attacker cannot attain the knowledge of the target model but only the confidence score $f_Y(X)$ with given input image X on the ground truth label Y . In our proposed method, we use confidence score as the adversarial loss. Thus, the objective is formalized as minimizing the confidence score on the ground truth label Y , shown as follows:

$$\begin{aligned} \arg \min_{\mathcal{G}_\theta} \mathbb{E}_{t \sim \mathcal{T}} [f_Y(t(X_{adv}, \mathcal{G}_\theta))] \\ \text{s.t. } f(X_{adv}) \neq Y \end{aligned} \quad (3)$$

AdvNB can be divided into two main parts: the digital-setting and the physical-setting. In the digital-setting, we generate adversarial samples by randomly generating adversarial neon beams with parameters L, R, I and C . In the physical-setting, we search for the most adversarial neon beams $\mathcal{G}_\theta = \{\theta_1, \theta_2, \dots, \theta_N\}$ using the confidence score $f_Y(X)$ and generate physical samples with function 2.

Algorithm 1 takes an input image X , ground truth label Y , a maximum number of iterations t_{max} , a maximum number of neon

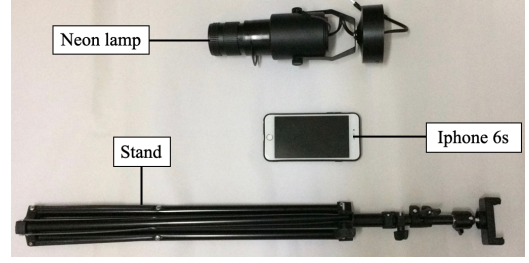


Figure 4: Experimental devices.

beams N , and a classifier f as input. At each iteration, the algorithm searches for the most adversarial neon beam $\theta(L, R, I, C)$ that generates an adversarial sample with the lowest confidence score $f_Y(X_{adv})$ on the ground truth label Y . It is important to note that a lower confidence score on the correct label of a digital sample indicates a more adversarial sample. The search terminates when the current X_{adv} is predicted with a label $argmax f(X_{adv}) \neq argmax f(X)$ or the maximum number of iterations t_{max} is reached. Finally, the algorithm outputs the physical parameters of the neon beams \mathcal{G}_θ , which are used to perform subsequent physical attacks.

4 EVALUATION

4.1 Experimental setting

We utilize ResNet50 [53] as the target model in all of our experimental tests, including digital and physical tests. Similar to the approach used in AdvLB [23], we randomly select 1000 images from ImageNet [54] that are correctly classified by ResNet50, with each image belonging to a different category, as our dataset for the digital test. In the physical test, the devices employed in our experiments are illustrated in Figure 4. The neon lamp can project various colors, such as red, green, blue, yellow, with four levels of intensity, ranging from 0.2 to 0.6. For the camera device, we use an iPhone6s, and it has been confirmed that the AdvNB is not affected by different camera devices. We use a maximum of 4 neon lamps for physical tests due to the limitation of the illuminated area. For all tests, we utilize attack success rate (ASR) as the metric to evaluate the effectiveness of AdvNB, which is defined as follows:

$$\begin{aligned} ASR(X) &= 1 - \frac{1}{O} \sum_{i=1}^O F(label_i) \\ F(label_i) &= \begin{cases} 1 & label_i \in L_{pre} \\ 0 & otherwise \end{cases} \end{aligned} \quad (4)$$

where O is the number of clean samples that can be correctly classified in the dataset X , $label_i$ represents the ground truth label of the i -th sample, L_{pre} is the set of all labels predicted under attacking.

4.2 Evaluation of effectiveness

Digital test: We conduct experiments in a digital setting using AdvNB on a dataset of 1000 images that were originally classified correctly by ResNet50. The results show an average ASR of 84.4% with 189.7 queries, using 20 neon beams with $R = 20$ pixels and $I = 0.7$. More digital attack results can be found in the supplementary

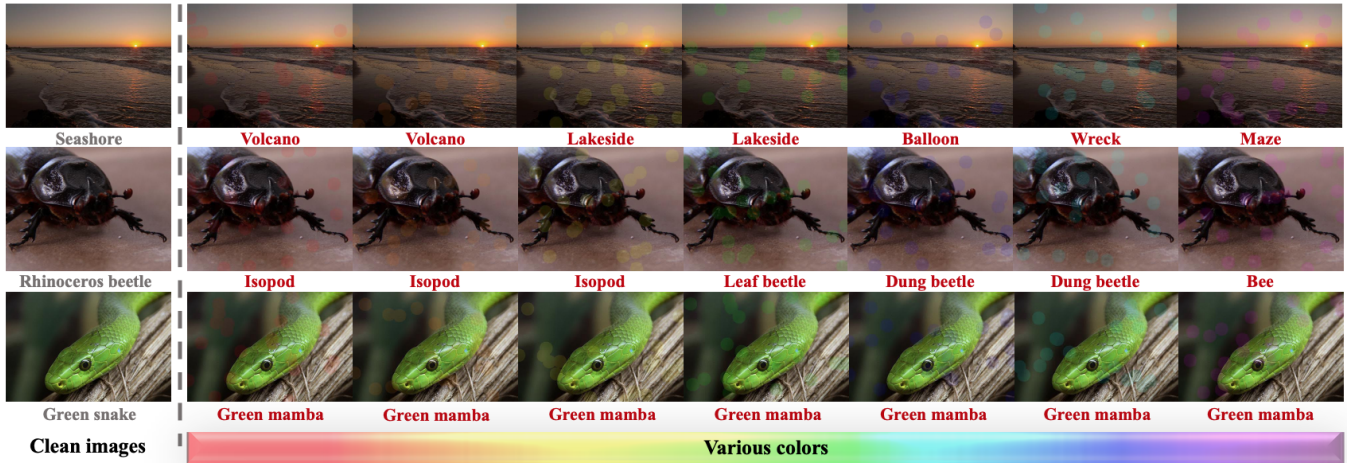


Figure 5: Adversarial samples generated by AdvNB. To validate the adversarial effectiveness of neon beams in the digital environment, we conduct experiments using neon beams of various colors, including red, orange, yellow, green, blue, indigo, and purple, to attack target model f . The results demonstrate that the target model failed to correctly classify digital samples with neon beams of different colors added.

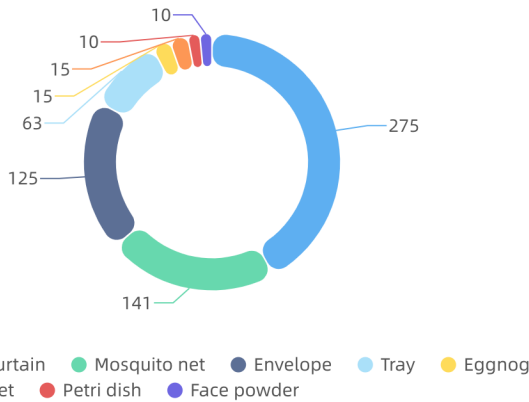


Figure 6: Statistics on misclassification of adversarial samples. Through statistical analysis of all the misclassification results, we can observe the semantic information categories that were most commonly associated with the adversarial neon beams.

materials. Figure 5 illustrates some interesting findings. The addition of neon beams of different colors to clean samples led the target model to misclassify the samples. For example, when neon beams are added to the "Seashore" image, the target model misclassify it as "Volcano", "Lakeside", "Balloon", and other categories. Although the adversarial neon beams in Figure 5 are perceptible to human observers, the semantic information of the adversarial samples is consistent with that of the clean samples. In fact, some of the adversarial samples are so subtle that the perturbations are not even noticeable upon a quick glance. Furthermore, we perform statistical analysis on the misclassification results of adversarial samples. Figure 6 shows that most of the digital samples are misclassified into a few categories such as "Shower curtain" and "Mosquito net". Therefore, we

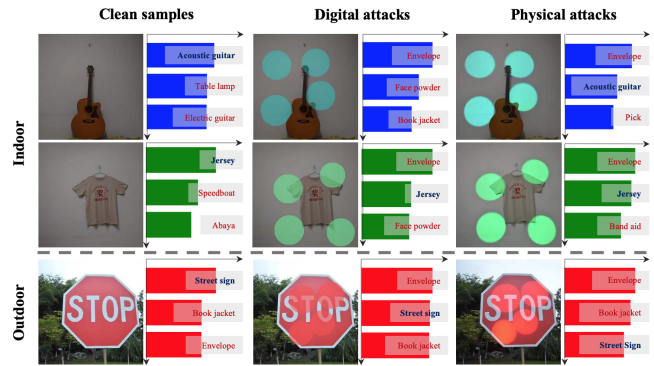


Figure 7: Indoor/outdoor test. The first column corresponds to the clean samples, the second column corresponds to the generated digital samples, and the third column corresponds to the generated physical samples after irradiation with neon beams. The bar chart presents the TOP-3 prediction labels of the target model and the corresponding confidence comparison. As shown, the physical and digital samples exhibit a high degree of consistency. Additionally, the TOP-1 classification results of physical samples by the target model match those of digital samples.

believe that the adversarial neon beam does not belong to any of the categories in ImageNet, but rather its semantic information is more similar to that of "Shower curtain" and "Mosquito net".

Physical test. We evaluate the efficacy of our proposed method in a physical setting, taking into account the potential impact of environmental noise on the effectiveness of physical attacks. To ensure the rigor of our experiments, we adopt a stringent experimental design that includes indoor and outdoor testing. The indoor test is

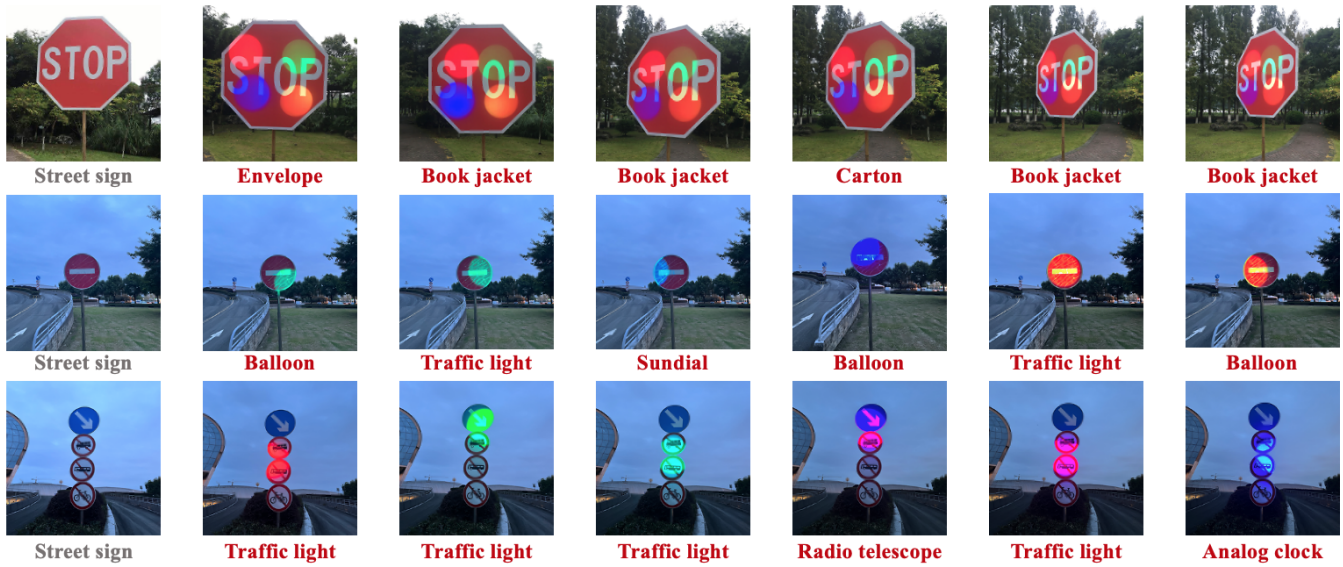


Figure 8: Physical samples. The top row of the figure displays the physical samples obtained by attacking the stop sign using neon beams at angles of 0° , 30° , and 45° . In the second and third row, we use a single neon beam to attack the road signs, leading to incorrect classification by the classifier.

Table 1: Comparison of experimental results between AdvIB and AdvLB.

Method	Digital		Physical		
	ASR(%)	Query	0° (%)	30° (%)	45° (%)
AdvLB [23]	95.1	834.0	77.4	\emptyset	\emptyset
AdvIB	84.4	189.7	100	100	33.3

designed to minimize the influence of outdoor noise, while the outdoor test aims to evaluate the performance of AdvNB in real-world scenarios.

For the indoor test, we select 'Acoustic guitar', 'Jersey', and other objects as targets, and generate 36 adversarial samples, achieving a 100% attack success rate (ASR of 100% in AdvLB [23]). The adversarial samples of the indoor test are presented in Figure 7, which shows that the computer-simulated neon beams maintain better consistency with the physical projected neon beams. In the outdoor test, we select "Street sign" as the attack object and form 132 adversarial samples, achieving an attack success rate of 81.82% (ASR of 77.43% in AdvLB [23]). Figure 8 displays the adversarial samples generated in the outdoor environment. Attackers can use the adversarial neon beams, as shown in Figure 8, to execute physical attacks that lead advanced DNNs to misclassify "Street sign" as "Envelope", "Book jacket", etc.

We summarize the experimental results of AdvLB and our proposed method in Table 1. As can be observed, in the digital environment, the ASR of our method is not superior to AdvLB, but our method exhibits significantly higher query efficiency than AdvIB. In the physical environment, our proposed method is capable of executing attacks from various angles, which is not feasible for AdvLB.

Furthermore, the physical ASR of our method is higher than that of AdvLB. Overall, our approach outperforms the baseline methods.

4.3 Evaluation of stealthiness

As previously stated, we choose neon beam as the physical perturbation in order to obtain a more natural physical sample, which makes our perturbation susceptible to being overlooked by human observers. As shown in Figure 8, our physical samples resemble natural neon beams falling on a street sign, and human observers have difficulty distinguishing between natural and artificial neon beams. On the other hand, the comparison of physical samples in Figure 2 shows that the physical perturbation generated by AdvNB is more stealthy than the baseline. Given AdvNB's light-speed attack, AdvNB has greater temporal stealthiness than RP2 [20] (RP2's physical perturbation will always adhere to the target object's surface, but AdvNB can control the light source, generating the physical perturbation only when the attack is carried out.). In contrast to AdvLB [23], the physical samples generated by AdvNB are more natural, allowing for better spatial stealthiness in our approach. When the cardboard is placed in front of the road sign for a shadow attack [25], it loses its spatial stealthiness, making human observers suspicious, whereas our method places the neon lamps far away from the target object, making AdvNB more stealthy than shadow attacks. In general, our approach results in a more stealthy attack than the baseline.

4.4 Evaluation of robustness

Deploy AdvNB to attack advanced DNNs. We evaluate the robustness of the proposed AdvNB in a black-box setting with various classifiers, including the advanced DNNs (Inception v3 [55], VGG19 [56], ResNet101 [53], GoogleNet [57], AlexNet [58], MobileNet [59], DenseNet [60], Augmix+ResNet50 [61], ResNet50+RS [62],

Table 2: Evaluation across various classifiers.

f	Top-1 Accuracy(%)	ASR(%)	Query
Inception v3	87.6	82.5	196.4
VGG19	91.5	89.6	157.2
ResNet101	96.1	81.3	209.7
GoogleNet	85.3	85.5	184.6
AlexNet	79.6	96.2	128.3
MobileNet	89.7	86.2	171.9
DenseNet	90.8	87.1	168.4
Augmix+ResNet50	93.7	79.8	221.6
ResNet50-RS	94.6	77.2	229.5
NF-ResNet50	94.8	76.4	237.8

Table 3: Transferability of AdvNB (ASR (%)).

f	Digital	Phy(0°)	Phy(30°)	Phy(45°)
Inception v3	75.9	77.8	39.5	4.5
VGG19	91.5	88.9	27.9	0
ResNet101	95.6	100	100	4.5
GoogleNet	79.7	80.0	55.8	22.7
AlexNet	95.1	100	100	79.5
MobileNet	85.4	86.7	44.2	20.5
DenseNet	76.9	82.2	51.2	20.5
Augmix+ResNet50	73.8	73.3	27.9	6.8
ResNet50-RS	71.4	77.8	44.2	9.1
NF-ResNet50	70.2	75.6	41.9	6.8

NF-ResNet50 [63]). Note that the dataset is 1000 images selected from ImageNet that can be correctly classified by ResNet50, the physical parameters for the adversarial neon beams are configured as follows: $N=20$, $I=0.7$, $R=20$ pixels. Table 2 shows the ASR of our method with different classifiers. AlexNet is found to be the most vulnerable in the black-box attack test, with a 96.2% ASR and an average of 128.3 queries. Furthermore, DNNs such as Augmix+ResNet50, ResNet50+RS, and NF-ResNet50 are more robust. In general, the data in Table 2 show that AdvNB have an adversarial effect of ASR on various models by more than 75% in the black-box setting, confirming the robustness of our proposed AdvNB.

Transferability of AdvNB. Here, we present the attack transferability of AdvNB to advanced DNNs [53, 55–63] in both digital and physical settings. We use the adversarial samples generated by AdvNB that successfully attacked resnet50 as the dataset. The experimental results are illustrated in Table 2. As shown, AdvNB exhibits excellent attack transferability in the digital environment, with an attack success rate above 90% against VGG19, ResNet101, and AlexNet. In the physical environment, AdvNB demonstrates outstanding attack transferability at 0°, which effectively paralyzes most advanced DNNs. These results suggest that AdvNB can be utilized by attackers to exploit the transferability of AdvNB for efficient physical attacks against advanced DNNs, without any prior knowledge of the target model.

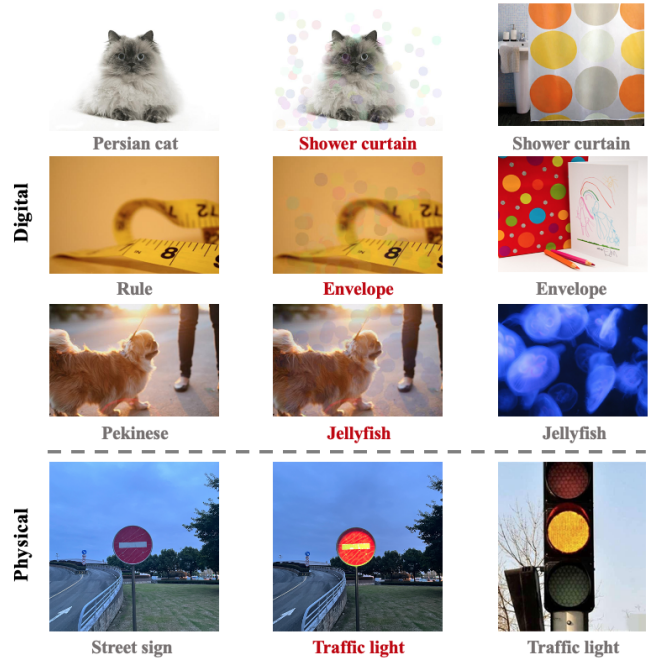


Figure 9: Prediction errors caused by AdvNB. The results of tests conducted in both digital and physical environments demonstrate that the adversarial neon beam contains semantic information pertaining to certain categories of objects, which hinders the classifier’s ability to accurately classify them.

The experimental results in Table 2 and Table 3 demonstrate that AdvNB conducts robust physical attacks in a black-box setting. AdvNB enables attackers to carry out flexible operations, without any knowledge of the model, to perform effective physical attacks. Therefore, considering the remarkable adversarial effect of AdvNB on the vision-based system in real scenes, we advocate for the attention and further exploration of the proposed AdvNB.

5 DISCUSSION

5.1 Analysis of prediction errors

The neon beams act as adversarial perturbations, altering the features of the original images and providing new cues to DNNs. As previously stated, the majority of the digital samples are misclassified as "Shower curtain", "Envelope", and so on. Figure 9 shows that the adversarial perturbations include several elements characteristic of a shower curtain. Additionally, our thorough analysis of the adversarial samples revealed some characteristic elements in "Envelope" that bear a strong resemblance to the perturbations. Moreover, single-color adversarial perturbations exhibit a significant similarity to "Jellyfish". In the physical experiment, we project a neon beam of color $C(255, 255, 0)$ onto a street sign, which the target model misclassified as a "Traffic light".

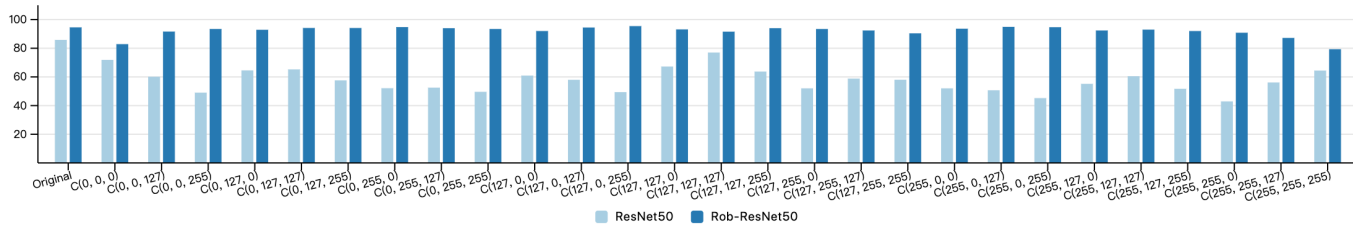


Figure 10: Defense of AdvNB. It is evident that Rob-ResNet50 can achieve a TOP-1 classification accuracy of over 80% for the 27 color adversarial samples, which is considered a basic level of adversarial defense. In fact, most defenses can achieve a TOP-1 classification accuracy of over 90%.

5.2 Defense of AdvNB

In addition to showcasing the potential threats posed by AdvNB, we also explore potential defense strategies against this attack, particularly through the use of adversarial training. To this end, we construct a larger dataset in order to rigorously study the efficacy of our proposed defense strategy. Our dataset, which we call ImageNet-NeonBeam (ImageNet-NB), comprises 1.35 million adversarial samples generated by adding 27 different colors of simulated neon beams with $N=20$, $I=0.7$, and $R=20$ pixels to each of the 50 randomly selected clean samples from each of the 1000 categories in ImageNet [54].

We utilize the torchvision framework to train a robust ResNet50 model, which is optimized on 3 2080Ti GPUs using the ADAM optimizer with an initial learning rate of 0.01. As depicted in Figure 10, the horizontal axis represents the various colors of neon beams added to the adversarial samples, and the vertical axis represents the corresponding TOP-1 classification accuracy. It is noteworthy that the robust model achieve a TOP-1 classification accuracy of over 90% in most cases. We subject Rob-ResNet50 to AdvNB attack, where we use $N=20$, $I=0.7$, and $R=20$ pixels, resulting in 70.7% ASR with an average query count of 353.8 (ResNet50: 84.4% ASR, 189.7 average queries). These results indicate that although adversarial training can reduce AdvNB’s ASR and increase AdvNB’s attack time cost, it is not a foolproof defense against AdvNB. Please refer to the supplementary material for additional experimental results on Rob-ResNet50.

5.3 Model attention

We utilize the Class Activation Mapping (CAM) technique [64] to visualize the model’s attention. In Figure 11, the first column displays the clean samples, while the third column displays the digital samples with the adversarial neon beam added to the upper left corner. A comparison of the second and fourth columns reveals that the model’s attention is disrupted when the adversarial neon beam is added to the corner of the clean sample.

6 CONCLUSION

In this work, we present a novel light-based physical attack called AdvNB that leverages the instantaneous nature of light to conduct effective physical attacks. Our evaluation criteria include effectiveness, stealthiness, and robustness. Extensive experimental designs and results demonstrate the effectiveness of AdvNB in both digital

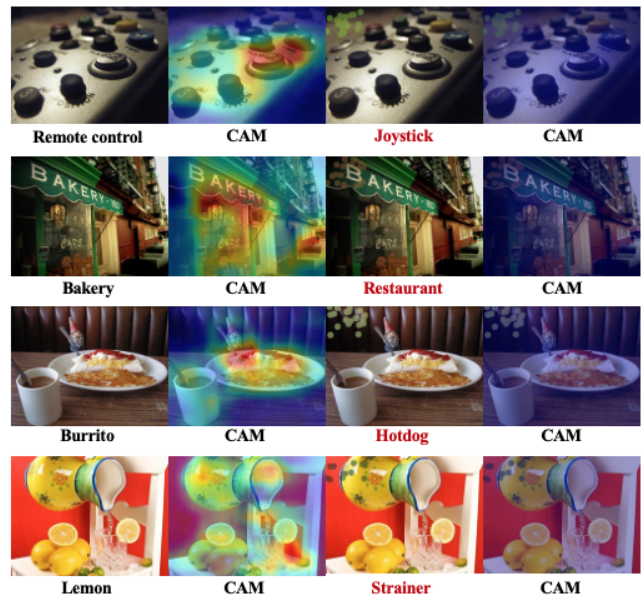


Figure 11: CAM for images.

and physical environments. We showcase the stealthiness of our proposed method in terms of both temporal and spatial stealthiness by comparing the generated physical sample with a baseline. We employ AdvNB to launch attacks on advanced DNNs, demonstrate the attack transferability of AdvNB to verify its robustness. Our research highlights the security threat posed by light-based physical attacks to the physical world and sheds new light on future physical attacks using light as physical perturbations instead of stickers to enhance the flexibility of physical attacks. The proposed AdvNB, as an effective, stealthy, and robust light-based physical attack, provides a valuable complement to recent physical attacks.

In future work, we plan to apply the proposed AdvNB to suit various tasks, including object detection and domain segmentation. We also aim to explore other light-based physical attacks, such as adversarial reflected light. Additionally, developing effective defense strategies against light-based attacks will be a promising research direction.

REFERENCES

- [1] A. Krizhevsky, I. Sutskever, and G. E. Hinton, "Imagenet classification with deep convolutional neural networks," *Advances in neural information processing systems*, vol. 25, pp. 1097–1105, 2012.
- [2] Q. V. Le, W. Y. Zou, S. Y. Yeung, and A. Y. Ng, "Learning hierarchical invariant spatio-temporal features for action recognition with independent subspace analysis," in *CVPR 2011*, pp. 3361–3368, IEEE, 2011.
- [3] Y. Taigman, M. Yang, M. Ranzato, and L. Wolf, "Deepface: Closing the gap to human-level performance in face verification," in *Proceedings of the IEEE conference on computer vision and pattern recognition*, pp. 1701–1708, 2014.
- [4] A. Geiger, P. Lenz, and R. Urtasun, "Are we ready for autonomous driving? the kitti vision benchmark suite," in *2012 IEEE conference on computer vision and pattern recognition*, pp. 3354–3361, IEEE, 2012.
- [5] T. P. Lillicrap, J. J. Hunt, A. Pritzel, N. Heess, T. Erez, Y. Tassa, D. Silver, and D. Wierstra, "Continuous control with deep reinforcement learning," in *4th International Conference on Learning Representations, ICLR 2016, San Juan, Puerto Rico, May 2-4, 2016, Conference Track Proceedings* (Y. Bengio and Y. LeCun, eds.), 2016.
- [6] F. Zhang, J. Leitner, M. Milford, B. Upcroft, and P. Corke, "Towards vision-based deep reinforcement learning for robotic motion control," *arXiv preprint arXiv:1511.03791*, 2015.
- [7] H. Bou-Ammar, H. Voos, and W. Ertel, "Controller design for quadrotor uavs using reinforcement learning," in *2010 IEEE International Conference on Control Applications*, pp. 2130–2135, IEEE, 2010.
- [8] C. Mostegel, M. Rumpfer, F. Fraundorfer, and H. Bischof, "Uav-based autonomous image acquisition with multi-view stereo quality assurance by confidence prediction," in *Proceedings of the IEEE Conference on Computer Vision and Pattern Recognition Workshops*, pp. 1–10, 2016.
- [9] C. Szegedy, W. Zaremba, I. Sutskever, J. Bruna, D. Erhan, I. J. Goodfellow, and R. Fergus, "Intriguing properties of neural networks," in *2nd International Conference on Learning Representations, ICLR 2014, Banff, AB, Canada, April 14-16, 2014, Conference Track Proceedings* (Y. Bengio and Y. LeCun, eds.), 2014.
- [10] N. Carlini and D. A. Wagner, "Adversarial examples are not easily detected: Bypassing ten detection methods," in *Proceedings of the 10th ACM Workshop on Artificial Intelligence and Security, AISec@CCS 2017, Dallas, TX, USA, November 3, 2017* (B. Thuraisingham, B. Biggio, D. M. Freeman, B. Miller, and A. Sinha, eds.), pp. 3–14, ACM, 2017.
- [11] N. Carlini and D. A. Wagner, "Towards evaluating the robustness of neural networks," in *2017 IEEE Symposium on Security and Privacy, SP 2017, San Jose, CA, USA, May 22-26, 2017*, pp. 39–57, IEEE Computer Society, 2017.
- [12] R. Duan, Y. Chen, D. Niu, Y. Yang, A. K. Qin, and Y. He, "Advdrop: Adversarial attack to dnns by dropping information," in *Proceedings of the IEEE/CVF International Conference on Computer Vision*, pp. 7506–7515, 2021.
- [13] Y. Dong, S. Cheng, T. Pang, H. Su, and J. Zhu, "Query-efficient black-box adversarial attacks guided by a transfer-based prior," *IEEE Transactions on Pattern Analysis and Machine Intelligence*, vol. 44, no. 12, pp. 9536–9548, 2021.
- [14] S. Feng, F. Feng, X. Xu, Z. Wang, Y. Hu, and L. Xie, "Digital watermark perturbation for adversarial examples to fool deep neural networks," in *2021 International Joint Conference on Neural Networks (IJCNN)*, pp. 1–8, IEEE, 2021.
- [15] X. Dong, D. Chen, J. Bao, C. Qin, L. Yuan, W. Zhang, N. Yu, and D. Chen, "Greedyfool: Distortion-aware sparse adversarial attack," in *Advances in Neural Information Processing Systems 33: Annual Conference on Neural Information Processing Systems 2020, NeurIPS 2020, December 6-12, 2020, virtual* (H. Larochelle, M. Ranzato, R. Hadsell, M. Balcan, and H. Lin, eds.), 2020.
- [16] B. G. Doan, M. Xue, S. Ma, E. Abbasnejad, and D. C. Ranasinghe, "Tnt attacks! universal naturalistic adversarial patches against deep neural network systems," *IEEE Transactions on Information Forensics and Security*, vol. 17, pp. 3816–3830, 2022.
- [17] X. Han, G. Xu, Y. Zhou, X. Yang, J. Li, and T. Zhang, "Physical backdoor attacks to lane detection systems in autonomous driving," in *Proceedings of the 30th ACM International Conference on Multimedia*, pp. 2957–2968, 2022.
- [18] X. Du and C.-M. Pun, "Adversarial image attacks using multi-sample and most-likely ensemble methods," in *Proceedings of the 28th ACM International Conference on Multimedia*, pp. 1634–1642, 2020.
- [19] S. Casper, M. Nadeau, D. Hadfield-Menell, and G. Kreiman, "Robust feature-level adversaries are interpretability tools," *Advances in Neural Information Processing Systems*, vol. 35, pp. 33093–33106, 2022.
- [20] K. Eykholt, I. Evtimov, E. Fernandes, B. Li, A. Rahmati, C. Xiao, A. Prakash, T. Kohno, and D. Song, "Robust physical-world attacks on deep learning visual classification," in *2018 IEEE Conference on Computer Vision and Pattern Recognition, CVPR 2018, Salt Lake City, UT, USA, June 18-22, 2018*, pp. 1625–1634, Computer Vision Foundation / IEEE Computer Society, 2018.
- [21] D. Song, K. Eykholt, I. Evtimov, E. Fernandes, B. Li, A. Rahmati, F. Tramèr, A. Prakash, and T. Kohno, "Physical adversarial examples for object detectors," in *12th USENIX Workshop on Offensive Technologies, WOOT 2018, Baltimore, MD, USA, August 13-14, 2018* (C. Rossow and Y. Younan, eds.), USENIX Association, 2018.
- [22] J. Li, F. R. Schmidt, and J. Z. Kolter, "Adversarial camera stickers: A physical camera-based attack on deep learning systems," in *Proceedings of the 36th International Conference on Machine Learning, ICML 2019, 9-15 June 2019, Long Beach, California, USA* (K. Chaudhuri and R. Salakhutdinov, eds.), vol. 97 of *Proceedings of Machine Learning Research*, pp. 3896–3904, PMLR, 2019.
- [23] R. Duan, X. Mao, A. K. Qin, Y. Chen, S. Ye, Y. He, and Y. Yang, "Adversarial laser beam: Effective physical-world attack to dnns in a blink," in *IEEE Conference on Computer Vision and Pattern Recognition, CVPR 2021, virtual, June 19-25, 2021*, pp. 16062–16071, Computer Vision Foundation / IEEE, 2021.
- [24] A. Sayles, A. Hooda, M. Gupta, R. Chatterjee, and E. Fernandes, "Invisible perturbations: Physical adversarial examples exploiting the rolling shutter effect," in *Proceedings of the IEEE/CVF Conference on Computer Vision and Pattern Recognition*, pp. 14666–14675, 2021.
- [25] Y. Zhong, X. Liu, D. Zhai, J. Jiang, and X. Ji, "Shadows can be dangerous: Stealthy and effective physical-world adversarial attack by natural phenomenon," in *Proceedings of the IEEE/CVF Conference on Computer Vision and Pattern Recognition*, pp. 15345–15354, 2022.
- [26] A. Athalye, L. Engstrom, A. Ilyas, and K. Kwok, "Synthesizing robust adversarial examples," in *Proceedings of the 35th International Conference on Machine Learning, ICML 2018, Stockholm, Sweden, July 10-15, 2018* (J. G. Dy and A. Krause, eds.), vol. 80 of *Proceedings of Machine Learning Research*, pp. 284–293, PMLR, 2018.
- [27] I. J. Goodfellow, J. Shlens, and C. Szegedy, "Explaining and harnessing adversarial examples," in *3rd International Conference on Learning Representations, ICLR 2015, San Diego, CA, USA, May 7-9, 2015, Conference Track Proceedings* (Y. Bengio and Y. LeCun, eds.), 2015.
- [28] S. Moosavi-Dezfooli, A. Fawzi, and P. Frossard, "Deepfool: A simple and accurate method to fool deep neural networks," in *2016 IEEE Conference on Computer Vision and Pattern Recognition, CVPR 2016, Las Vegas, NV, USA, June 27-30, 2016*, pp. 2574–2582, IEEE Computer Society, 2016.
- [29] J. Su, D. V. Vargas, and K. Sakurai, "One pixel attack for fooling deep neural networks," *IEEE Trans. Evol. Comput.*, vol. 23, no. 5, pp. 828–841, 2019.
- [30] S. Moosavi-Dezfooli, A. Fawzi, O. Fawzi, and P. Frossard, "Universal adversarial perturbations," in *2017 IEEE Conference on Computer Vision and Pattern Recognition, CVPR 2017, Honolulu, HI, USA, July 21-26, 2017*, pp. 86–94, IEEE Computer Society, 2017.
- [31] B. Bonnet, T. Furon, and P. Bas, "Generating adversarial images in quantized domains," *IEEE Transactions on Information Forensics and Security*, vol. 17, pp. 373–385, 2021.
- [32] Q. Li, Y. Qi, Q. Hu, S. Qi, Y. Lin, and J. S. Dong, "Adversarial adaptive neighborhood with feature importance-aware convex interpolation," *IEEE Transactions on Information Forensics and Security*, vol. 16, pp. 2447–2460, 2020.
- [33] H. Hosseini and R. Poovendran, "Semantic adversarial examples," in *2018 IEEE Conference on Computer Vision and Pattern Recognition Workshops, CVPR Workshops 2018, Salt Lake City, UT, USA, June 18-22, 2018*, pp. 1614–1619, Computer Vision Foundation / IEEE Computer Society, 2018.
- [34] A. S. Shamsabadi, R. Sánchez-Matilla, and A. Cavallaro, "Colorfool: Semantic adversarial colorization," in *2020 IEEE/CVF Conference on Computer Vision and Pattern Recognition, CVPR 2020, Seattle, WA, USA, June 13-19, 2020*, pp. 1148–1157, Computer Vision Foundation / IEEE, 2020.
- [35] Z. Zhao, Z. Liu, and M. A. Larson, "Towards large yet imperceptible adversarial image perturbations with perceptual color distance," in *2020 IEEE/CVF Conference on Computer Vision and Pattern Recognition, CVPR 2020, Seattle, WA, USA, June 13-19, 2020*, pp. 1036–1045, Computer Vision Foundation / IEEE, 2020.
- [36] Z. Hu, S. Huang, X. Zhu, F. Sun, B. Zhang, and X. Hu, "Adversarial texture for fooling person detectors in the physical world," in *Proceedings of the IEEE/CVF Conference on Computer Vision and Pattern Recognition*, pp. 13307–13316, 2022.
- [37] J. Wang, A. Liu, Z. Yin, S. Liu, S. Tang, and X. Liu, "Dual attention suppression attack: Generate adversarial camouflage in physical world," in *IEEE Conference on Computer Vision and Pattern Recognition, CVPR 2021, virtual, June 19-25, 2021*, pp. 8565–8574, Computer Vision Foundation / IEEE, 2021.
- [38] N. Suryanto, Y. Kim, H. Kang, H. T. Larasati, Y. Yun, T.-T.-H. Le, H. Yang, S.-Y. Oh, and H. Kim, "Dta: Physical camouflage attacks using differentiable transformation network," in *Proceedings of the IEEE/CVF Conference on Computer Vision and Pattern Recognition*, pp. 15305–15314, 2022.
- [39] D. Wang, T. Jiang, J. Sun, W. Zhou, Z. Gong, X. Zhang, W. Yao, and X. Chen, "FCA: learning a 3d full-coverage vehicle camouflage for multi-view physical adversarial attack," in *Thirty-Sixth AAAI Conference on Artificial Intelligence, AAAI 2022, Thirty-Fourth Conference on Innovative Applications of Artificial Intelligence, IAAI 2022, The Twelfth Symposium on Educational Advances in Artificial Intelligence, EAAI 2022 Virtual Event, February 22 - March 1, 2022*, pp. 2414–2422, AAAI Press, 2022.
- [40] X. Zeng, C. Liu, Y. Wang, W. Qiu, L. Xie, Y. Tai, C. Tang, and A. L. Yuille, "Adversarial attacks beyond the image space," in *IEEE Conference on Computer Vision and Pattern Recognition, CVPR 2019, Long Beach, CA, USA, June 16-20, 2019*, pp. 4302–4311, Computer Vision Foundation / IEEE, 2019.
- [41] H. D. Liu, M. Tao, C. Li, D. Nowrouzezahrai, and A. Jacobson, "Beyond pixel norm-balls: Parametric adversaries using an analytically differentiable renderer,"

- in *7th International Conference on Learning Representations, ICLR 2019, New Orleans, LA, USA, May 6-9, 2019*, OpenReview.net, 2019.
- [42] J. Liu, B. Lu, M. Xiong, T. Zhang, and H. Xiong, "Adversarial attack with raindrops," *arXiv preprint arXiv:2302.14267*, 2023.
- [43] L. Zhai, F. Juefei-Xu, Q. Guo, X. Xie, L. Ma, W. Feng, S. Qin, and Y. Liu, "Adversarial rain attack and defensive deraining for dnn perception," *arXiv preprint arXiv:2009.09205*, 2022.
- [44] A. Kurakin, I. J. Goodfellow, and S. Bengio, "Adversarial examples in the physical world," in *5th International Conference on Learning Representations, ICLR 2017, Toulon, France, April 24-26, 2017, Workshop Track Proceedings*, OpenReview.net, 2017.
- [45] X. Wei, Y. Guo, and J. Yu, "Adversarial sticker: A stealthy attack method in the physical world," *IEEE Transactions on Pattern Analysis and Machine Intelligence*, 2022.
- [46] K. Xu, G. Zhang, S. Liu, Q. Fan, M. Sun, H. Chen, P. Chen, Y. Wang, and X. Lin, "Adversarial t-shirt! evading person detectors in a physical world," in *Computer Vision - ECCV 2020 - 16th European Conference, Glasgow, UK, August 23-28, 2020, Proceedings, Part V* (A. Vedaldi, H. Bischof, T. Brox, and J. Frahm, eds.), vol. 12350 of *Lecture Notes in Computer Science*, pp. 665–681, Springer, 2020.
- [47] R. Wang, F. Juefei-Xu, Q. Guo, Y. Huang, X. Xie, L. Ma, and Y. Liu, "Amora: Black-box adversarial morphing attack," in *Proceedings of the 28th ACM International Conference on Multimedia*, pp. 1376–1385, 2020.
- [48] S. Chen, C. Cornelius, J. Martin, and D. H. P. Chau, "Shapeshifter: Robust physical adversarial attack on faster R-CNN object detector," in *Machine Learning and Knowledge Discovery in Databases - European Conference, ECML PKDD 2018, Dublin, Ireland, September 10-14, 2018, Proceedings, Part I* (M. Berlingerio, F. Bonchi, T. Gärtner, N. Hurley, and G. Ifrim, eds.), vol. 11051 of *Lecture Notes in Computer Science*, pp. 52–68, Springer, 2018.
- [49] S. Huang, X. Liu, X. Yang, and Z. Zhang, "An improved shapeshifter method of generating adversarial examples for physical attacks on stop signs against faster r-cnns," *Comput. Secur.*, vol. 104, p. 102120, 2021.
- [50] R. Duan, X. Ma, Y. Wang, J. Bailey, A. K. Qin, and Y. Yang, "Adversarial camouflage: Hiding physical-world attacks with natural styles," in *2020 IEEE/CVF Conference on Computer Vision and Pattern Recognition, CVPR 2020, Seattle, WA, USA, June 13-19, 2020*, pp. 997–1005, Computer Vision Foundation / IEEE, 2020.
- [51] A. Gnanasambandam, A. M. Sherman, and S. H. Chan, "Optical adversarial attack," in *IEEE/CVF International Conference on Computer Vision Workshops, ICCVW 2021, Montreal, BC, Canada, October 11-17, 2021*, pp. 92–101, IEEE, 2021.
- [52] A. Guesmi, M. A. Hanif, and M. Shafique, "Advrain: Adversarial raindrops to attack camera-based smart vision systems," *arXiv preprint arXiv:2303.01338*, 2023.
- [53] K. He, X. Zhang, S. Ren, and J. Sun, "Deep residual learning for image recognition," in *2016 IEEE Conference on Computer Vision and Pattern Recognition, CVPR 2016, Las Vegas, NV, USA, June 27-30, 2016*, pp. 770–778, IEEE Computer Society, 2016.
- [54] J. Deng, W. Dong, R. Socher, L. Li, K. Li, and L. Fei-Fei, "Imagenet: A large-scale hierarchical image database," in *2009 IEEE Computer Society Conference on Computer Vision and Pattern Recognition (CVPR 2009), 20-25 June 2009, Miami, Florida, USA*, pp. 248–255, IEEE Computer Society, 2009.
- [55] C. Szegedy, V. Vanhoucke, S. Ioffe, J. Shlens, and Z. Wojna, "Rethinking the inception architecture for computer vision," in *2016 IEEE Conference on Computer Vision and Pattern Recognition, CVPR 2016, Las Vegas, NV, USA, June 27-30, 2016*, pp. 2818–2826, IEEE Computer Society, 2016.
- [56] K. Simonyan and A. Zisserman, "Very deep convolutional networks for large-scale image recognition," in *3rd International Conference on Learning Representations, ICLR 2015, San Diego, CA, USA, May 7-9, 2015, Conference Track Proceedings* (Y. Bengio and Y. LeCun, eds.), 2015.
- [57] C. Szegedy, W. Liu, Y. Jia, P. Sermanet, S. E. Reed, D. Anguelov, D. Erhan, V. Vanhoucke, and A. Rabinovich, "Going deeper with convolutions," in *IEEE Conference on Computer Vision and Pattern Recognition, CVPR 2015, Boston, MA, USA, June 7-12, 2015*, pp. 1–9, IEEE Computer Society, 2015.
- [58] A. Krizhevsky, I. Sutskever, and G. E. Hinton, "Imagenet classification with deep convolutional neural networks," in *Advances in Neural Information Processing Systems 25: 26th Annual Conference on Neural Information Processing Systems 2012. Proceedings of a meeting held December 3-6, 2012, Lake Tahoe, Nevada, United States* (P. L. Bartlett, F. C. N. Pereira, C. J. C. Burges, L. Bottou, and K. Q. Weinberger, eds.), pp. 1106–1114, 2012.
- [59] M. Sandler, A. G. Howard, M. Zhu, A. Zhmoginov, and L. Chen, "Mobilenetv2: Inverted residuals and linear bottlenecks," in *2018 IEEE Conference on Computer Vision and Pattern Recognition, CVPR 2018, Salt Lake City, UT, USA, June 18-22, 2018*, pp. 4510–4520, Computer Vision Foundation / IEEE Computer Society, 2018.
- [60] G. Huang, Z. Liu, L. van der Maaten, and K. Q. Weinberger, "Densely connected convolutional networks," in *2017 IEEE Conference on Computer Vision and Pattern Recognition, CVPR 2017, Honolulu, HI, USA, July 21-26, 2017*, pp. 2261–2269, IEEE Computer Society, 2017.
- [61] D. Hendrycks, N. Mu, E. D. Cubuk, B. Zoph, J. Gilmer, and B. Lakshminarayanan, "Augmix: A simple data processing method to improve robustness and uncertainty," in *8th International Conference on Learning Representations, ICLR 2020, Addis Ababa, Ethiopia, April 26-30, 2020*, OpenReview.net, 2020.
- [62] I. Bello, W. Fedus, X. Du, E. D. Cubuk, A. Srinivas, T. Lin, J. Shlens, and B. Zoph, "Revisiting resnets: Improved training and scaling strategies," in *Advances in Neural Information Processing Systems 34: Annual Conference on Neural Information Processing Systems 2021, NeurIPS 2021, December 6-14, 2021, virtual* (M. Ranzato, A. Beygelzimer, Y. N. Dauphin, P. Liang, and J. W. Vaughan, eds.), pp. 22614–22627, 2021.
- [63] A. Brock, S. De, S. L. Smith, and K. Simonyan, "High-performance large-scale image recognition without normalization," in *Proceedings of the 38th International Conference on Machine Learning, ICML 2021, 18-24 July 2021, Virtual Event (M. Meila and T. Zhang, eds.)*, vol. 139 of *Proceedings of Machine Learning Research*, pp. 1059–1071, PMLR, 2021.
- [64] B. Zhou, A. Khosla, À. Lapedriza, A. Oliva, and A. Torralba, "Learning deep features for discriminative localization," in *2016 IEEE Conference on Computer Vision and Pattern Recognition, CVPR 2016, Las Vegas, NV, USA, June 27-30, 2016*, pp. 2921–2929, IEEE Computer Society, 2016.